

Targeted Fast Frequency Response by Decomposing Frequency into Transient and Steady-State Deviations

J. Sánchez Cortés, *Graduate Student Member, IEEE*, M. Rezaei Jegarluei, and S. Azizi, *Senior Member, IEEE*
School of Electronic and Electrical Engineering, University of Leeds, Leeds LS2 9JT, UK
eljsc@leeds.ac.uk; elmri@leeds.ac.uk; s.azizi@leeds.ac.uk

Abstract— The increasing penetration of renewable energy sources (RESs) into power systems is reducing the effectiveness of operation, control, and protection schemes traditionally employed in power systems. The decoupling of RESs' kinetic energy from the rest of the system and, thus, the variability of system inertia pose a critical challenge to maintaining frequency stability. In this paper, a new paradigm is set forth for optimal fast-acting frequency containment (OFFC) through a short yet targeted active power injection. This concept builds upon the innovative idea of decomposing frequency response into transient and steady-state deviations. The core aim of OFFC is to reduce or completely remove the transient frequency deviation without unnecessarily changing the settling frequency. This minimizes the time and efforts required to restore the frequency within the statutory limit while avoiding unnecessary expenditure of turbines' lifetime. Only after allocating enough resources for removing the transient deviation, the system operators may utilize the remaining power resources (if any) to reduce the steady-state deviation. The system frequency response (SFR) model and the loss of generation size are needed as input to formulate the shape, time, and volume of the targeted injection required. This is readily accomplished by applying the inverse SFR model to the frequency correction required. Extensive simulations conducted on the IEEE 39-bus test system verify the effectiveness and reliability of the proposed method for OFFC.

Keywords—Optimal fast-acting frequency containment (OFFC), targeted power injection, frequency decomposition, renewable energy sources.

I. INTRODUCTION

Renewable energy sources (RESs) are increasingly integrated into power systems to meet ambitious decarbonization targets worldwide. This transition is necessary yet introduces new operational issues due to the intermittent nature of RESs and their indirect connection to the system via inverter-based interfaces. A resulting challenge is the variability of the system inertia in an unprecedented wide range [1], where system inertia can be considered the system stiffness against loss of generation (LoG) events. This is why the increasing penetration of RESs amplifies the unpredictability and variability of the frequency response [2].

The constancy of system frequency is a measure of the balance between active power generation and consumption. LoG events disrupt this balance, which leads to a decrease in frequency that can be decomposed into transient and steady-state frequency deviations. The steady-state deviation refers to the difference between the pre-event and settling frequencies. In this paper, the frequency deviation below the settling frequency

is referred to as transient frequency deviation. The lowest frequency reached is called frequency nadir. If the frequency falls below the statutory limit, e.g., 1% of the nominal frequency [3], steam turbines will receive accumulative damage that will reduce their lifetime. When the frequency decline is not arrested fast enough, local protection systems will disconnect generators to prevent frequency from reaching the resonant frequencies of steam turbine blades [4]. Therefore, failure to timely arrest frequency decline will result in further LoG events and eventually a blackout.

To preserve the power system integrity against LoG events, fast recovery of the active power balance is necessary. This can be achieved by resorting to under-frequency load shedding (UFLS) or fast active power injection. UFLS schemes regain the power balance by disconnecting an appropriate amount of load from the system [4]. Although load shedding is not a desirable solution, UFLS occasionally becomes the last resort against system collapse as conventional generating units lack the capability of fast power injection (contrary to RESs). Conventional UFLS relays drop a predefined amount of load every time the local frequency violates a frequency threshold. This makes the process relatively slow in arresting the frequency decline [5]. Adaptive UFLS schemes are set forth to accelerate load shedding, thus avoiding low-frequency nadirs. To calculate the LoG size, these schemes usually rely upon the swing equation and the rate of change of frequency (RoCoF) [6], [7]. However, in systems with volatile inertia, a high RoCoF is no longer an indicator of a larger LoG event, which is different from the case in conventional power systems [8]. The volatility of system inertia makes adaptive UFLS schemes unable to reliably estimate the LoG size, thus, less effective.

The ability to quickly adjust the output power of generating units is essential for effectively counteracting frequency deviations following LoG events. RESs are not inherently responsive to frequency deviations because they are connected to the power grid through power electronic interfaces. This, along with the limited capacity of RESs to inject extra power, makes frequency containment challenging in the short timeframe available before frequency drops significantly. Despite these challenges, RESs offer great potential that can resolve the foregoing shortcomings if used properly. Fast-acting frequency containment (FFC) refers to applying the extra power of RESs to mitigate frequency deviations. FFC is faster than the primary control of synchronous generators (SGs). This is because controlling the output of power electronic devices is typically much faster than the response time of SGs [9], [10].

Conventional fast-acting frequency containment (CFFC) has been traditionally designed to imitate the frequency response of SGs or to act as a step-function-shaped injection counteracting the LoG event. In this context, the extra power injection by RESs should have a fast ramp-up rate with a small delay and be sustained for enough time to mitigate frequency deviations [9]. References [11]–[13] propose a controller that mimics the frequency regulation capability of SGs. Other researchers in [14]–[18] investigate approaches to deliver extra active power from batteries, super-capacitors, and HVDC links.

Some CFFC techniques focus on the kinetic energy stored in wind turbine rotors to slow the frequency decline following an LoG event. The primary challenge these methods try to address is the fact that the rotor speed of wind turbines is only allowed to decelerate to a limited extent [19]. If not appropriately moderated, this may give rise to a frequency second dip, which may lead to even a lower frequency nadir [20]. References [14], [15], [20]–[24] focus on preventing the frequency second dip while improving the frequency nadir using energy storage systems. However, these solutions are less attractive for practical applications due to the high cost and large-scale capacity requirements [22]. CFFC solutions, in principle, strive to shift the entire frequency response upward uniformly. In other words, these methods treat the transient and steady-state frequency deviations as an indivisible entity. This paper will show that this is not an optimal solution, for it does not lead to the highest frequency nadir. It is shown that CFFC may even unnecessarily increase the duration required for the frequency to return within the statutory limit.

A core contribution of this paper is to highlight the significance of and the need for ensuring the treatment of the transient frequency deviation before focusing on the steady-state frequency deviation. The paper proposes optimal fast-acting frequency containment (OFFC) as a technique for targeting the extra power injections at delivering the highest possible frequency nadir. OFFC maximizes the effectiveness of available resources, as will be justified mathematically and verified using extensive simulations. Contrary to common belief in the power systems community, this extra injection should not resemble a step function and is not even expected to be maintained permanently. Rather it is injected in a specific shape and at a particular time, for it is targeted at removing the transient deviation. OFFC reduces the time to return the frequency within the statutory limit without any unrealistic assumptions on the technology readiness or capability of available resources.

The remainder of this paper is structured as follows. Section II puts forward a novel idea to decompose the frequency response into transient and steady-state deviations. This is shown to be necessary for producing the highest frequency nadir. The concept and relevance of triangular-shaped extra injection are detailed and discussed in Section III. The proposed idea is validated through extensive simulations in Section IV. Section V summarizes the findings and conclusions drawn from the research work.

II. OPTIMAL FAST-ACTING FREQUENCY CONTAINMENT

In this section, the frequency response following an LoG event is decomposed into transient and steady-state frequency

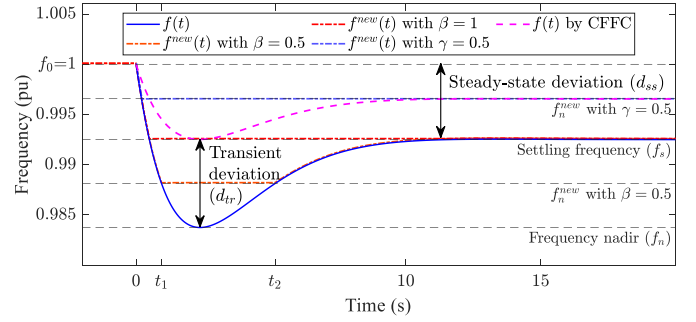


Fig. 1. Frequency containment by decomposing frequency response into transient and steady-state deviations.

deviations. This decomposition is the basis for OFFC, which results in the optimal frequency response with the highest frequency nadir. In doing so, the system frequency response (SFR) model [4] is used to establish a link between the available fast-acting injections from RESs and the fraction of the transient frequency deviation that such injections can counteract. If appropriately implemented, OFFC ensures that the frequency of the center of inertia (CoI) will remain constant for a few seconds and then begin to ascend to the settling frequency.

A. Decomposition of Frequency Response

Following an LoG event, the CoI frequency begins and continues to decrease unless the power generation and consumption in the system match again. This equilibrium of power, as described by the swing equation, results in a RoCoF of zero. This is when the frequency response reaches its nadir. On the other hand, the response of turbine governors of SGs increases their power injection. The increase in power generation by SGs helps frequency recover its settling value, which is ideally within the statutory limit, as shown in Fig. 1.

The depth of the frequency deviation can be attributed to the superposition of the depths caused by transient and steady-state components, which are short-lived and permanent, respectively. This decomposition is based on the SFR model, which is a second-order minimum-phase transfer function in its simplified form. Fig. 1 shows the decomposition of a typical frequency response following an LoG event. Separating transient and steady-state frequency deviations is key to optimal frequency containment using fast-acting power resources.

The steady-state frequency deviation is defined as the difference between the nominal and settling frequencies. This quantity is determined by the LoG size and the settings of the turbine governors of the remaining SGs [4]. The depth of the transient deviation measures the distance between the settling frequency and the frequency nadir. The failure to promptly mitigate the transient frequency deviation and violating the frequency statutory limit increases the gradual accumulation of irreversible damage in steam turbines. Depending on the extent and duration of the under-frequency condition, the UFLS scheme may also be triggered to arrest the excessive frequency decline and avert the risk of a blackout.

It will be shown in this section that a targeted short-term compensation of the generation deficit will be far more effective/useful in containing system frequency than any

constant deployment of available resources of extra power. The remainder of this paper is aimed at formulating the short-term extra power injection to remove the transient deviation partially/completely. Indeed, the entire transient frequency deviation can be effectively mitigated when sufficient extra power is delivered by RESs for a short period of time. In cases where the available extra power is not large enough, it can be optimally deployed so as to reduce the depth of transient frequency deviation as much as possible. This approach results in the highest frequency nadir for any available extra power.

B. Optimality of Flattened Frequency Response

The blue curve $f(t)$ in Fig. 1 is a generic curve demonstrating how the CoI frequency responds to an LoG event and begins to deviate from its original value of f_0 . In its trajectory, $f(t)$ drops to a nadir of f_n and then recovers to the settling frequency f_s . In this figure, the depths of transient and steady-state frequency deviations are marked by d_{tr} and d_{ss} and are equal to $f_s - f_n$ and $f_0 - f_s$, respectively. Now, let us assume some extra power is injected such that the desired frequency response $f^{new}(t)$ becomes flattened in part (or from one instance onwards), examples of which are shown by dash-dotted curves in Fig. 1. Let us define the transient correction β as a real number (between 0 and 1) indicating the portion of the depth of transient frequency deviation that is to be removed by OFFC. It follows that $\beta = 0$ for the original frequency response. The enhanced frequency responses shown in dash-dotted orange and red curves are associated with $\beta = 0.5$ and $\beta = 1$, respectively.

Without loss of generality, the desired frequency response is assumed to be flattened for $t_1 \leq t \leq t_2$ and to coincide with the original frequency response elsewhere. $\Delta p(t)$ is the extra active power injection resulting in the enhanced frequency response whose nadir is denoted by f_n^{new} . Therefore, $E = \int_0^\infty \Delta p(t) dt$ is the net energy required to achieve this enhanced frequency response. We show that the energy needed to achieve any frequency response lying above the flattened frequency response (with the same or higher nadirs) is certainly greater than E . The flattened frequency response is considered optimal in the sense that reaching a frequency nadir higher than f_n^{new} requires a larger amount of energy to be injected.

The power system is supposed to be a linear time-invariant system in terms of power-frequency relationship. This is a convenient way of representing the differential equations governing the system frequency dynamics. The average course of the CoI frequency response to changes in generation/load can be approximated by a second-order model that retains enough details without losing essential dynamic characteristics [25]. The LoG size is assumed to be known to the control center within 0.5 sec following the LoG inception [8], [26]. Let us use $F(s)$, $P(s)$ and $G_{SFR}(s)$ to denote the frequency response, power disturbance, and SFR transfer function in the Laplace domain, respectively. With these, frequency can be written as

$$F(s) = P(s) \times G_{SFR}(s) \quad (1)$$

where the SFR transfer function can be approximated as [25]

$$G_{SFR}(s) = \left(\frac{R\omega_n^2}{DR + K_m} \right) \left(\frac{1 + T_R s}{s^2 + 2\zeta\omega_n s + \omega_n^2} \right) \quad (2)$$

where parameters R , D , K_m , T_R , ζ , and ω_n respectively represent the effects of the governor droop, frequency dependence of load, mechanical gain factor, reheat time constant, damping factor, and natural frequency of the system.

Let $f(t)$, $p(t)$, and $g_{SFR}(t)$ be the time domain functions of the frequency response, power disturbance, and SFR model, respectively. In the time domain, the convolution of the input power and SFR transfer function describes the output frequency as below [27]:

$$f(t) = (p * g_{SFR})(t) = f_0 + \int_0^\infty p(\tau) g_{SFR}(t - \tau) d\tau \quad (3)$$

where the symbol $*$ represents the convolution operation of two functions and can be seen as a measure expressing how the course of one function is modified by the other one. The convolution of two functions in the time domain is equivalent to the inverse Laplace transform of the product of the Laplace transforms of the two functions [27].

Writing a similar equation as (3) for the enhanced frequency $f^{new}(t)$ and subtracting the two equations gives

$$\overbrace{f^{new}(t) - f(t)}^{\Delta f(t)} = \int_0^\infty \overbrace{(p^{new}(\tau) - p(\tau))}^{\Delta p(\tau)} g_{SFR}(t - \tau) d\tau \quad (4)$$

where $\Delta f(t)$ is the frequency correction needed to achieve $f^{new}(t)$.

Based on Fubini's theorem and convolution properties, the integral of the convolution of two functions on the whole space is equal to the product of their integrals (each over the whole space) [27], [28]. The original integral limits span from negative to positive infinity. However, the lower limit can be adjusted to 0, knowing that the power system is a causal system in which there cannot be a response prior to the input. Hence,

$$\overbrace{\int_0^\infty \Delta f(t) dt}^{\text{Extent of recovered deviation}} = \overbrace{\int_0^\infty \Delta p(t) dt}^{\text{Injected energy}} \overbrace{\int_0^\infty g_{SFR}(\tau) d\tau}^{R/(DR + K_m)} \quad (5)$$

Since $\Delta f(t)$ takes non-zero values only between t_1 and t_2 and is zero otherwise, the lower and upper integral limits in (5) can be changed to t_1 and t_2 , respectively. The left-hand side of (5) is the area between the original and enhanced frequency responses. The first integral on the right-hand side of (5) represents the energy injected to ensure the intended frequency response. The second integral represents the area under the impulse response of the system. Equation (5) is general and can be extended to the removal of all or a portion of the steady-state deviation once the entire d_{tr} is removed. The steady-state correction extent is shown by γ and takes a real value between 0 and 1. A steady-state correction of γ means that that γd_{ss} is removed from the steady-state deviation.

III. TARGETED ACTIVE POWER INJECTION

In this section, the extra injection profile is obtained as a function of the LoG size, correction extent, and SFR model. It is shown that this injection is not a step function but almost triangular, contrary to the LoG event, which is a step reduction in generation. The LoG size is assumed to be available in the

control center by directly monitoring the generator's circuit breakers. Otherwise, it can be estimated using the PMU data received from the wide-area monitoring system [8].

Let us assume the LoG event in per unit can be modeled as a negative step function with magnitude P . Given the SFR transfer function (2), the system frequency in the time domain is obtained to be [4]

$$f(t) = f_0 - \frac{RP}{DR+K_m} [1 + \alpha e^{-\zeta\omega_n t} \sin(\omega_r t + \phi)] \quad (6)$$

where α , ω_r , and ϕ are constants determined based on the SFR model parameters as detailed in [25]. The first two terms on the right-hand side of (6) define the settling frequency f_s as below:

$$f_s = f_0 - \frac{RP}{DR+K_m} \quad (7)$$

The original frequency nadir is obtained by evaluating (6) when the frequency derivative becomes zero for the first time at [25]

$$t_n = \frac{1}{\omega_r} \tan^{-1} \left(\frac{\omega_r T_R}{\zeta \omega_n T_R - 1} \right) \quad (8)$$

which means $f_n = f(t_n)$. Let us assume that β portion of this transient deviation is to be removed. This means the new frequency nadir is $f_n^{new} = \beta d_{tr} + f_n$, and the enhanced frequency response can be expressed as

$$f^{new}(t) = \begin{cases} f(t) & t < t_1 \text{ and } t_2 < t \\ \beta d_{tr} + f_n & t_1 \leq t \leq t_2 \end{cases} \quad (9)$$

This enhanced frequency response is flattened from t_1 to t_2 and coincides with the original frequency response elsewhere. From (9), one can easily conclude that t_1 and t_2 are the first and second positive roots of the equation below:

$$f(t) - (\beta d_{tr} + f_n) = 0 \quad (10)$$

Let $u(t)$ be the unit-step function occurring at $t = 0$. With the definitions just put forward and based on (9), the frequency correction needed is

$$\Delta f(t) = (f_n^{new} - f(t))(u(t - t_1) - u(t - t_2)) \quad (11)$$

The next step is to obtain the extra injection to ensure $f^{new}(t)$ from $\Delta P(s) = \Delta F(s)/G_{SFR}(s)$. By computing the inverse Laplace transform of $\Delta P(s)$, one can easily derive $\Delta p(t)$.

Fig. 2 shows the $\Delta p(t)$ needed for removing 20%, 50%, and 80% of the depth of transient deviation of the frequency response shown in Fig. 1. It can be easily demonstrated that, in general, the extra injection needed can be approximated with two triangles, regardless of the value of β . In this paper, and for simplicity, the second triangle, which is much smaller, is dropped as this does not significantly impact the enhanced frequency response.

Only when the sum of available resources is sufficient for a complete transient compensation ($\beta = 1$); the remaining power could also be appropriately injected to remove part of the steady-state deviation. In doing so, a similar formulation can be derived to correct a fraction of the steady-state frequency deviation depth. As mentioned, γ denotes the portion of the steady-state frequency deviation to be removed after the complete removal

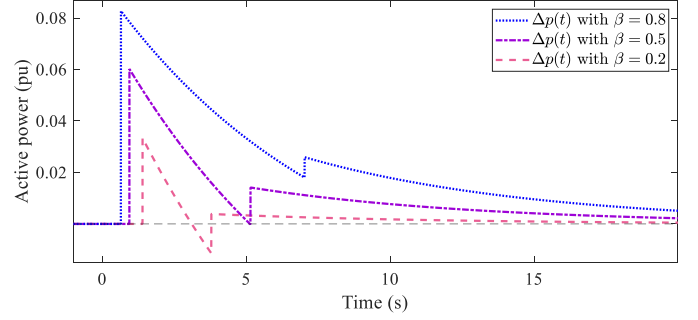


Fig. 2. Extra injection needed for removing transient frequency deviation.

TABLE I
SFR MODELS FOR THE IEEE 39-BUS TEST SYSTEM

Base case	Light-load	Heavy-load
$\left(\frac{0.015(1 + 2.15s)}{s^2 + 0.3s + 0.46^2} \right)$	$\left(\frac{0.019(1 + 1.88s)}{s^2 + 0.29s + 0.49^2} \right)$	$\left(\frac{0.018(1 + 3.39s)}{s^2 + 0.38s + 0.44^2} \right)$

of the transient deviation. Since the new frequency nadir is $f_n^{new} = f_s + \gamma d_{ss}$, the enhanced frequency response is

$$f^{new}(t) = \begin{cases} f(t) & t < t_1 \\ f_s + \gamma d_{ss} & t \geq t_1 \end{cases} \quad (12)$$

One may desire to flatten the frequency response from t_1 onward if the available resources from RESs exceed the amount needed to recover the entire transient frequency deviation. In these cases, the time to start injecting power is the positive root of the equation below:

$$f(t) - (f_s + \gamma d_{ss}) = 0 \quad (13)$$

Then, the frequency correction needed is calculated from

$$\Delta f(t) = (f_n^{new} - f(t))u(t - t_1) \quad (14)$$

Again, the extra injection to ensure $f^{new}(t)$ is obtained from $\Delta P(s) = \Delta F(s)/G_{SFR}(s)$. By computing the inverse Laplace transform of $\Delta P(s)$, one can easily derive $\Delta p(t)$.

IV. PERFORMANCE EVALUATION

In this section, the effectiveness of the proposed method is evaluated by conducting an extensive number of simulations on the IEEE 39-bus test system in DIGSILENT PowerFactory. A general performance evaluation demonstrates the method's capability to provide FFC against LoG events considering various control settings for RESs. Then, the effectiveness of the extra injections in maximizing the frequency nadir is studied under different loading conditions. Finally, a comparative analysis is conducted between the proposed OFFC and the CFFC methods.

A. System Frequency Response Model Derivation

To evaluate the method's performance, the SFR model of the IEEE 39-bus test system is required. To obtain the SFR model, an offline study is carried out by tripping SGs while RESs are operated in the constant power mode. The CoI frequency is then computed for each LoG event, and the Curve Fitting Toolbox of MATLAB is employed to estimate the parameters of (2). The average of estimates for each parameter is utilized to derive the

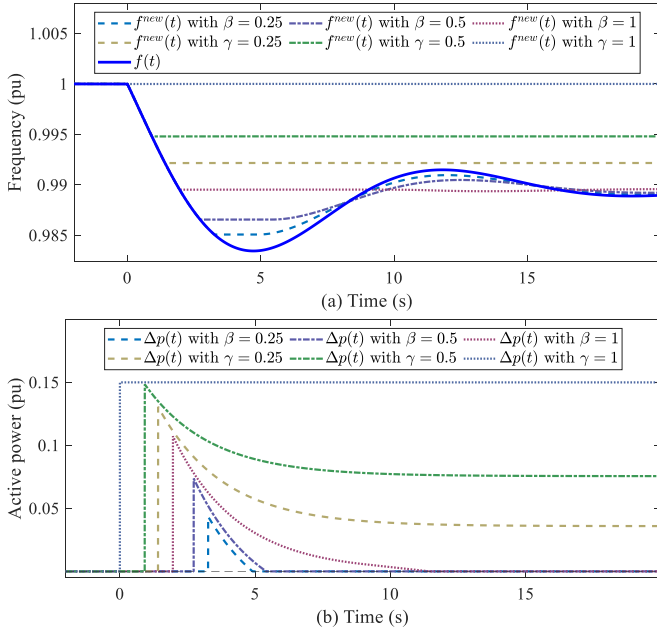


Fig. 3. Impact of different correction extents on (a) Enhanced frequency response achieved, and (b) Extra power injections required.

representative SFR model of the IEEE 39-bus test system. The SFR model is developed for three different loading conditions. To create each scenario, a 50% increase and decrease are uniformly applied to the load/generation of the base case system. This allows for examining the system's response under light-load and heavy-load conditions, as well. The SFR models of these scenarios are summarized in Table I.

B. General Performance Analysis

Twenty randomly distributed RESs are added to the IEEE 39-bus test system. Without loss of generality, all RESs share identical characteristics, including a nominal power rating of 250 MVA, active power setpoint of $P_{ref} = 0.68$ pu, and reactive power setpoint of $Q_{ref} = 0.076$ pu. These settings represent a 50% RES penetration level and serve as the base case. To assess the effectiveness of the proposed method, a 930-MW outage scenario is examined using the base case SFR model reported in Table I. Fig. 3(a) shows the enhanced frequency responses where the transient and steady-state frequency deviations are removed to different extents. The corresponding extra injections required to achieve these frequency responses are illustrated in Fig. 3(b). As can be seen, achieving the maximum frequency nadir requires injecting a smaller amount of active power than the size of the LoG event. The targeted injection does not resemble a step function contrary to the LoG event. The extra injections with non-zero γ consist of two components. The first component is a so-called triangle-shaped injection aimed at removing the entire transient deviation. This is essentially a short-lived energy injection. The second component is a sustained power injection for correcting the corresponding portion of the steady-state deviation.

In compliance with [29], the maximum ramp-up and ramp-down rates of RESs are assumed to be 500 ms. The effect of this on OFFC is evaluated for a 700-MW LoG event. Fig. 4 shows

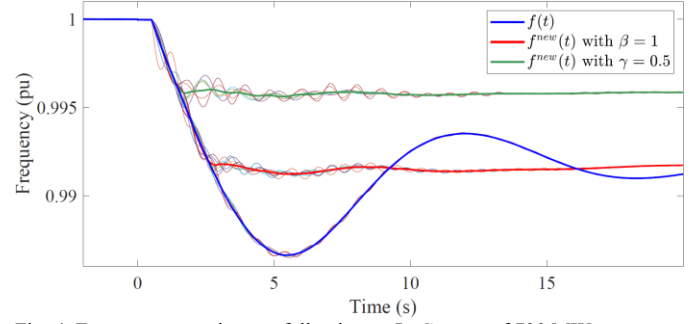


Fig. 4. Frequency containment following an LoG event of 700 MW.

TABLE II
SENSITIVITY OF FREQUENCY NADIR TO SETTINGS, NUMBER, AND LOCATIONS OF RESs FOLLOWING A 600-MW LOG EVENT

RES Penetration Level	12 RESs	15 RESs	20 RESs	25 RESs
	CoI Frequency Nadir (Hz)			
50%	49.55	49.53	49.57	49.63
60%	49.55	49.59	49.59	49.61
70%	49.51	49.6	49.58	49.62

the frequency response for two different extents of frequency deviation removal. The thick red curve represents the complete removal of the transient deviation, whereas the thick green curve corresponds to the removal of half of the steady-state deviation. The thin curves depict local frequency responses, whose frequency nadirs might be slightly lower than that of the CoI frequency. This is because local and inter-area oscillations are averaged out in the CoI frequency. Nevertheless, the CoI frequency is regarded as a valuable tool, for it provides a holistic picture of system frequency behavior following an LoG event.

The proposed method's robustness is assessed by varying RESs number, locations, and control settings within a wide range. The increase in RES generation is proportionally deducted from SGs to maintain the total system generation constant. By randomly changing the RES locations, each scenario is simulated 100 times, and the obtained results are averaged. Table II summarizes the CoI frequency nadir for a 600-MW LoG event under different RES penetration levels. The RES injections are targeted at completely removing the transient frequency deviation. As can be seen, the fast-acting contribution of RESs contains the frequency nadir above the statutory limit regardless of the penetration level and location of RESs.

C. OFFC versus CFFC

In this subsection, the performances of OFFC and CFFC (step power injection) are compared. Fig. 5 shows the frequency nadir as a function of the total energy injected for a 1000-MW LoG event. As expected, OFFC results in higher frequency nadirs, regardless of the amount of energy injected. Table III presents the energy required to contain the frequency nadir above the statutory limit for 20 seconds. This is carried out for different LoG events, with an RES penetration level of 50%. The results confirm that in comparison with CFFC, OFFC requires significantly less energy to maintain frequency within the statutory limits.

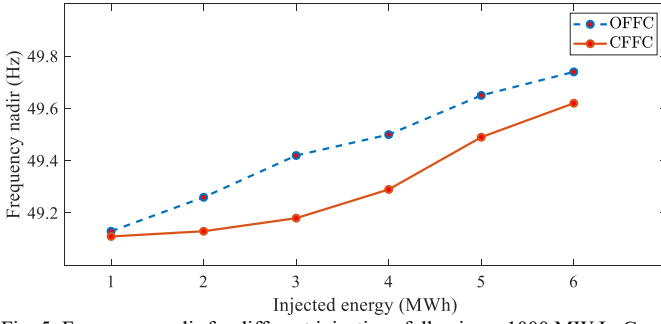


Fig. 5. Frequency nadir for different injections following a 1000 MW LoG.

TABLE III
ENERGY NEEDED TO CONTAIN FREQUENCY WITHIN STATUTORY LIMITS

LoG Size (MW)	Energy Required (MWh)	
	CFFC	OFFC
600	0.25	0.04
800	1.34	0.29
1000	2.42	1.15
1200	3.51	2.22

V. CONCLUSION

This paper sets forth a new paradigm for optimal fast-acting frequency containment (OFFC) by decomposing the frequency response into transient and steady-state deviations. This lays the foundation for deriving the optimal size, shape, and time for extra power injections upon a loss of generation (LoG) event. It is shown that, contrary to common belief, the extra injection should not be a step function counteracting the event unless the amount of power resources available is as large as the LoG size. A smaller yet well-timed triangular injection is shown to be the optimal injection for maximizing the frequency nadir, as justified mathematically, and supported by extensive simulations. It is concluded that targeting the extra injection at the removal of transient frequency deviation increases the extent of improvement made by a given amount of energy. Only after the complete removal of the transient deviation, the remaining resources are allowed to be allocated to the removal of steady-state deviation. This is key to minimizing the time/energy needed to effectively bring the frequency back within the statutory limits with minimal efforts and preserve the lifespan of equipment such as steam turbines.

REFERENCES

- [1] A. Ulbig, T. Borsche and G. Andersson, "Impact of low rotational inertia on power system stability and operation," *IFAC Proceedings Volumes*, vol. 47, no. 3, p. 7290-7297, 2014.
- [2] P. Tielens and D. V. Hertem, "The relevance of inertia in power systems," *Renewable and Sustainable Energy Reviews*, vol. 55, pp. 999 – 1009, 2016. [Online] Available: <https://doi.org/10.1016/j.rser.2015.11.016>
- [3] National Grid ESO, "The grid code, Issue 6, Revision 12", Great Britain, Mar. 2022, [Online] Available: <https://www.nationalgrideso.com>
- [4] P. M. Anderson, *Power System Protection*, New York: IEEE Press, 1999.
- [5] MIGRATE, "Development and tests of new protection solutions when reaching 100% PE penetration," EU H2020 MIGRATE Project, Deliverable 4.3, Tech. Rep., Dec. 2018.
- [6] M. Sun, G. Liu, M. Popov, V. Terzija and S. Azizi, "Underfrequency load shedding using locally estimated RoCoF of the center of inertia," *IEEE Trans. Power Syst.*, vol. 36, no. 5, pp. 4212-4222, Sept. 2021.

- [7] S. Azizi, M. Sun, G. Liu and V. Terzija, "Local frequency-based estimation of the rate of change of frequency of the center of inertia," *IEEE Trans. Power Syst.*, vol. 35, no. 6, pp. 4948-4951, Nov. 2020.
- [8] J. Sanchez Cortes, M. R. Jegarlupei, P. Aristidou, K. Li and S. Azizi, "Size/location estimation for loss of generation events in power systems with high penetration of renewables," *Electric Power Systems Research*, vol. 219, 2023.
- [9] GE Grid Solutions, "Enhanced frequency control capability (EFCC), optimization detailed design," NG-EFCC-SPEC-004 v1, Tech. Rep., Jan. 2016.
- [10] Y. Cheng, R. Azizipah, S. Azizi, L. Ding and V. Terzija, "Smart frequency control in low inertia energy systems based on frequency response techniques: A review," *Applied Energy*, vol. 279, 2020.
- [11] W. He, X. Yuan and J. Hu, "Inertia provision and estimation of PLL-based DFIG wind turbines," *IEEE Trans. Power Syst.*, vol. 32, no. 1, pp. 510-521, Jan. 2017.
- [12] L. Harnefors *et al.*, "Generic PLL-based grid-forming control," *IEEE Trans. Power Electron.*, vol. 37, no. 2, pp. 1201-1204, Feb. 2022.
- [13] X. Guo *et al.*, "Inertial PLL of grid-connected converter for fast frequency support," *CSEE Journal of Power and Energy Systems*, pp. 1–6, 2022.
- [14] C. Zhang, E. Rakhshani, N. Veerakumar, J. L. R. Torres and P. Palensky, "Modeling and optimal tuning of hybrid ESS supporting fast active power regulation of fully decoupled wind power generators," *IEEE Access*, vol. 9, pp. 46409-46421, 2021.
- [15] J. Lee *et al.*, "Analytical approach for fast frequency response control of VSC HVDC," *IEEE Access*, vol. 9, pp. 91303-91313, 2021.
- [16] M. M. Kabsha and Z. H. Rather, "A new control scheme for fast frequency support from HVDC connected offshore wind farm in low-inertia system," *IEEE Trans. Sust. Energy*, vol. 11, no. 3, pp. 1829-1837, July 2020.
- [17] K. Jose, O. Adeyemi, J. Liang and C. E. Ugalde-Loo, "Coordination of fast frequency support from multi-terminal HVDC grids," *2018 IEEE International Energy Conference (ENERGYCON)*, 2018, pp. 1-6.
- [18] O. Stanojev *et al.*, "Enhanced MPC for fast frequency control in inverter-dominated power systems," *2020 International Conference on Smart Energy Systems and Technologies (SEST)*, 2020, pp. 1-6.
- [19] D. Yang, L. Hua and X. Zhang, "Fast frequency support of a DFIG based on over-speed de-loaded curve," *2021 IEEE/IAS Industrial and Commercial Power System Asia (I&CPS Asia)*, 2021, pp. 1314-1318.
- [20] X. Zhao, Y. Xue and X. -P. Zhang, "Fast frequency support from wind turbine systems by arresting frequency nadir close to settling frequency," *IEEE Open Access Journal of Power and Energy*, vol. 7, pp. 191-202, 2020.
- [21] G. Xu, L. Xu and J. Morrow, "System frequency support using wind turbine kinetic energy and energy storage system," *2nd IET Renewable Power Generation Conference (RPG 2013)*, 2013, pp. 1-4.
- [22] K. Sun *et al.*, "Frequency compensation control strategy of energy storage in the wind-energy storage hybrid system for improving frequency response performance," *2019 IEEE Industry Applications Society Annual Meeting*, 2019, pp. 1-8.
- [23] W. Liu, G. Geng, Q. Jiang, H. Fan and J. Yu, "Model-free fast frequency control support with energy storage system," *IEEE Trans. Power Syst.*, vol. 35, no. 4, pp. 3078-3086, July 2020.
- [24] Y. Yoo, S. Jung and G. Jang, "Dynamic inertia response support by energy storage system with renewable energy integration substation," *Journal of Modern Power Systems and Clean Energy*, vol. 8, no. 2, pp. 260-266, March 2020.
- [25] P. M. Anderson and M. Mirheydar, "A low-order system frequency response model," *IEEE Trans. Power Syst.*, vol. 5, no. 3, pp. 720-729, Aug. 1990.
- [26] S. Azizi, M. R. Jegarlupei, A. S. Dobakhshari, G. Liu and V. Terzija, "Wide-area identification of the size and location of loss of generation events by sparse PMUs," *IEEE Trans. on Power Delivery*, vol. 36, no. 4, pp. 2397-2407, Aug. 2021.
- [27] R. N. Bracewell, *The Fourier Transform and its Applications*, New York: McGraw-Hill, 1986.
- [28] A. Aksoy, and M. Martelli, "Mixed partial derivatives and Fubini's theorem," *College Mathematics Journal of MAA*, vol. 33, 2002.
- [29] National Grid ESO, "Dynamic containment response balancing service", Test Guidance for Providers, Great Britain, Jun. 2022.